BV Cen: A Possible Type 1a Supernova Progenitor?

Jordan Shaw
Supervisor: Dr Chris Watson
Queen's University Belfast
School of Mathematics and Physics

ABSTRACT

If a white dwarf in a cataclysmic variable binary system is a progenitor of type 1a supernovae, it must have a mass greater than that of an isolated white dwarf and close to the Chandrasekhar limit. The mass ratio of the long period dwarf nova BV Cen was estimated using rotational broadening and radial velocity of the donor star, and the radial velocity of emission lines arising from the white dwarf's surrounding accretion disc. The spectra used were from a MIKE echelle spectrograph data taken over 3 nights on a Magellan 6.5m telescope. The most reliable method means of determining the mass ratio is using radial velocity and rotational broadening of the donor. The rotational broadening $vsini$was estimated to be (96.0±2.0) kms^{-1} using an iterative process of cross-correlation with a non-rotating G8IV template and optimal subtraction. A mass ratio of (0.899±0.029) was found using the donor star radial velocity curve and therefore produced a white dwarf mass of (1.17±0.23)$M_{\odot}$. This mass is higher than the mass of an isolated white dwarf, 0.7$M_{\odot}$ and therefore confirms that the white dwarf has gained mass by accretion. The high mass estimate with associated uncertainty suggests that the white dwarf may reach the Chandrasekhar mass limit and explode as a type 1a supernova. However mass loss by nova and dwarf nova eruptions may prevent the white dwarf from reaching M_{Ch}. The low mass ratio suggests stability of mass transfer. The white dwarf mass estimate is in agreement with the previously calculated value of (1.18±0.28)$M_{\odot}$ by Watson et al, 2007 [1] to within the stated uncertainty.

1. INTRODUCTION

1.1 Type 1a Supernovae

Stars undergoing an explosion during which their luminosity becomes comparable to an entire galaxy are known as supernovae. Supernovae are classified according to their observed properties [2]. The main distinguishing characteristic is that type II supernovae display hydrogen lines in their spectra, while type I do not. Type I supernovae are also subdivided according to their spectra, with only type 1a supernovae (SNIa) displaying a silicon absorption line at 6150Å. Only type 1b (SNIb) display He I absorption lines while type 1c (SNIc) show an absence of both features

Type 1a supernovae (SNIa) are important in cosmology. There is a correlation between the decline rate of their light curves and their absolute magnitudes [3]. This has led to SNIa being the preferred 'standard candle' to determine cosmological distances.
A progenitor of SNIa has yet to be satisfactorily explained. The widely accepted view is that the supernova is formed from thermonuclear explosions of carbon-oxygen white dwarfs (WD) in close binary systems [4]. This is supported by the fact that the amount of energy observed in supernova explosions is equal to the energy produced in the conversion of carbon and oxygen to iron [5]. For carbon ignition to be triggered the mass of the white dwarf must approach Chandrasekhar mass. This is the mass at which the star can no longer be supported by electron degeneracy pressure, around 1.44$M_{\odot}$[6]. However the nature of the companion in the binary system is still uncertain [4].

One model is that the companion is another white dwarf. This is known as the Double Degenerate Model (DDM). In the DDM the two carbon-oxygen white dwarfs have a combined mass greater than or equal to M_{Ch}. Gravitational wave radiation reduces their orbital separation leading to their merger and explosion in the form of a SNIa [6].

Another model is that the white dwarf accretes material from a non-degenerate companion and approaches M_{Ch}. Before the white dwarf can undergo gravitational collapse, carbon fusion begins in the core and causes a thermonuclear explosion producing the SNIa [7].

One candidate for the non-degenerate companion in this model is a class of binary known as a Cataclysmic Variable (CV). These binary systems involve short orbital periods typically ranging from 1 hour to 14 hours. The close proximity of the secondary star in orbit around the white dwarf causes it to be tidally distorted due to the gravitational effect of the white dwarf, fill its Roche Lobe and begin to lose material to the WD through the inner Lagrangian point. The extreme tides cause the rotational period to lock to the orbital period and circularise the orbit.
If the white dwarf does not possess a strong magnetic field the material will form an accretion disc orbiting the WD. Strongly magnetic WDs disrupt accretion disc formation if the magnetic pressure is greater than the ram pressure of the accretion stream. This can lead to polar systems, where the WD accretes along magnetic field lines, or the formation of a truncated disc (intermediate polars).

Cataclysmic Variables are so named because of their sudden and often dramatic variations in brightness due to various phenomena. The two most dramatic of these phenomena are known as nova and dwarf nova eruptions [8][9].
Nova eruptions occur when accreted material builds up on the WD surface forming a layer. The density and temperature of this layer increases until fusion is triggered. The envelope expands rapidly and material is ejected. Eruptions occur with typically 6-19 magnitudes and last weeks to months.
Dwarf nova eruptions are much more common than nova eruptions and occur when the amount of material in the accretion disc reaches a critical mass. Instability leads to rapid accretion through the disc onto the WD surface and an expansion of the disc. A dramatic brightening of the disc occurs due to liberation of gravitational potential energy in the form of heat and light. The outbursts typically are of 2-6 magnitudes and with recurrence times of weeks to months. As dwarf nova eruptions only occur in systems with accretion discs, non-magnetic CVs are termed 'dwarf novae'.
These phenomena cause the mass of the white dwarf to be reduced, but do not permanently disrupt the binary, therefore they are classed as 'cataclysmic.'

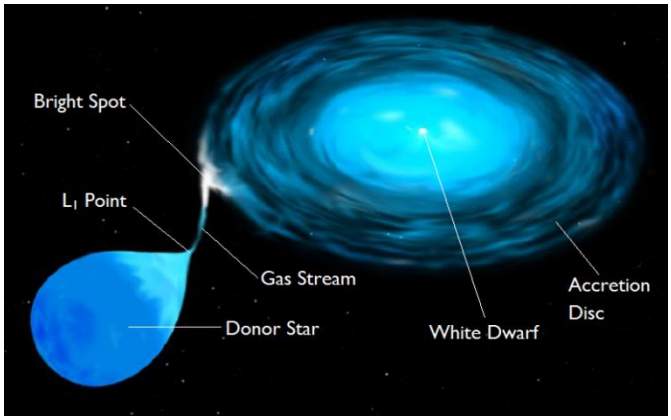

Fig. 1 The structure of a cataclysmic variable such as BV Cen

BV Centauri (BV Cen) is an eclipsing, binary system consisting of a secondary star which is evolved slightly from the main sequence in orbit around a white dwarf with orbital period (and also rotational period) of around 14 hours 40 minutes. It is a non-magnetic system and therefore classed as a 'dwarf nova'.

1.2 Objectives

The purpose of this project was to determine whether the white dwarf in BV Cen is particularly high- greater than that of an isolated white dwarf, typically around $0.7M_{\odot}$[10]. This would lend evidence for the white dwarf gaining mass from the donor and potentially reaching Chandrasekhar mass, making it a possible SNIa progenitor.
The mass ratio of the binary is given by equation (1).

$$q = \frac{M_2}{M_1} = \frac{K_1}{K_2} \qquad \textit{Equation (1)}$$

Where: M_1 and M_2 are the masses of the white dwarf and the donor star respectively

K_1 and K_2 are the radial velocity semi-amplitudes of the white dwarf and donor star respectively

Two estimates were calculated for the mass ratio q using the radial velocity curves of the two components of BV Cen. The estimates were found using the rotational broadening and radial velocity of the donor star, and the radial velocity motion of emission lines from the accretion disc surrounding the white dwarf.

2. EXPERIMENTAL DATA

2.1 Observations

The experimental data was taken using the Clay Magellan 6.5m telescope at Las Campanas, Chile. The telescope is an alt-azimuth design with principal foci at $\frac{f}{11}$ at the two Nasmyth locations and $\frac{f}{15}$ in the Cassegrain position.
Spectra from BV Cen were taken using a high resolution double echelle spectrograph MIKE (Magellan Inamori Kyocera Echelle) at the Nasmyth port. MIKE observes in the blue (typically 320-480nm) and red (typically 440-1000nm) channels which are recorded on separate CCDs (Charge Coupled Devices). Observations were made over three nights, giving six sets of data in total [11]

The data was reduced to files containing the spectra which could be analysed using the Linux software package 'molly.'
63 usable spectra were taken in the red arm- 22 from night 1, 20 from night 2 and 21 from night 3. Only spectra taken in the red arm were used in this investigation. The BV Cen donor star is observed in the red due to its relatively low temperature of 5000-6000K in comparison with the hotter white dwarf companion.

2.2 Rotational Broadening

When handling spectral data from BV Cen it must be noted that absorption lines from the donor star have been rotationally broadened.
Since CVs are tidally synchronised this means the donor star rotates once per orbit. In the case of BV Cen this means that the donor star rotates roughly every 14 hours 40 minutes, equal to its orbital period. This rapid rotation causes Doppler broadening of spectral lines from the star. Atoms contributing to spectral lines have differing line-of-sight velocities so that their individual contributions are shifted from their normal wavelength by differing amounts. From BV Cen spectral line contributions from both approaching and receding portions of the star are seen simultaneously. Approaching sections are blue-shifted and receding sections red-shifted. This is known as rotational broadening. The total absorption in each line is not affected by the broadening, so as a line becomes wider, it also becomes shallower [12].

When measuring radial velocities the axis of rotation will be inclined to our line-of-sight, and so the inclination i of the system must be accounted for. There is a projection effect of $sini$, meaning if i is not known, all that can be measured is the projected equatorial velocity, $vsini$ [13].

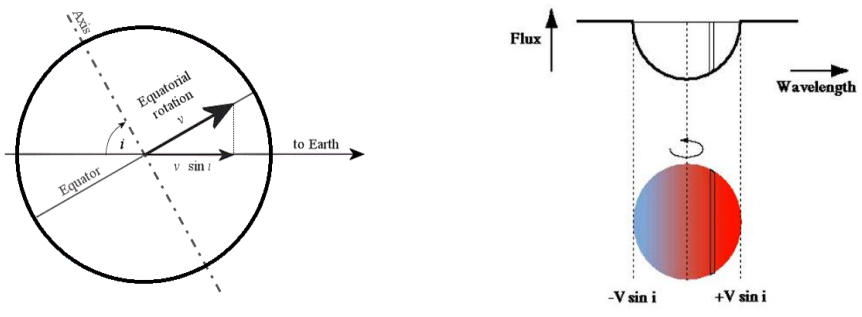

Fig. 2 and 3: The projected equatorial velocity and rotational broadening of spectral lin

3. ROTATIONAL BROADENING OF ABSORPTION LINE PROFILES OF ORDINARY STAR

3.1 Normalisation of Data

Fig. below shows a colour representation (trail) of night 1 data, where darker areas represent absorption lines and light regions represent emission lines. The continuum, or general count level, of the spectra vary from exposure to exposure. This is due to various reasons. The alt-azimuth telescope tracks the star precisely as it moves across the sky due to the rotation of the earth. Therefore small variations in the earth's rotation will change the amount of sunlight entering the slit. The earth's atmosphere and passing clouds may reduce the amount of starlight entering the slit and cause variations in the point spread function of the star. Variations could also be due to natural changes in the brightness of the star itself from its accretion regions.

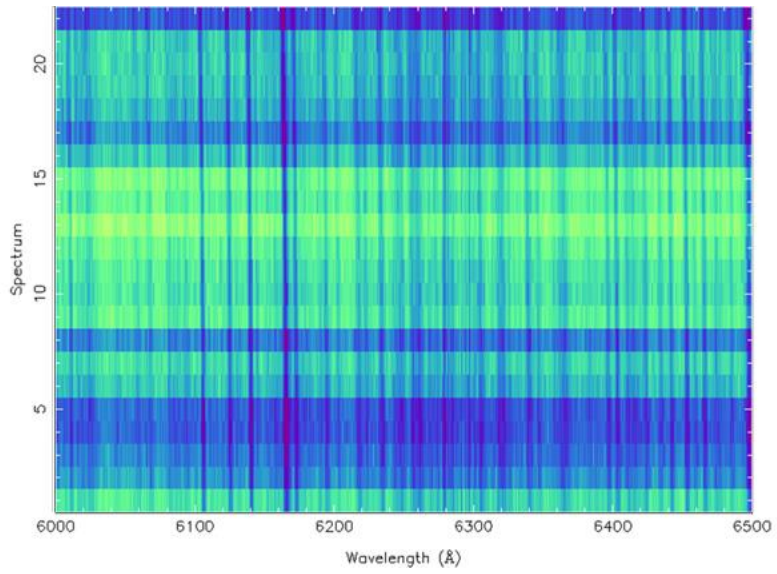

Fig.4: Night 1 spectra before normalisation

In order to remove the continuum variations, the spectra were normalised in the region of interest. The donor star absorption spectra were used in the wavelength range 6000-6500Å. This region displays temperature and gravity sensitive absorption lines from the donor star, free from lines from accretion regions.
Data points were clipped from each end of the spectra to ensure that the only data used was within the range 6000-6500Å. Third order polynomials were fit to each spectrum.
By changing the upper and lower reject thresholds data points could be excluded from the fit. For all three nights the upper reject threshold was set to 3 standard deviations. For night 1 the lower reject threshold for all spectra was 1.1σ, for night 2 1.2σ and night 3 1.3σ.
The continuum fits were checked for each spectrum and each night. Each spectrum was then normalised by dividing by the polynomial fit.

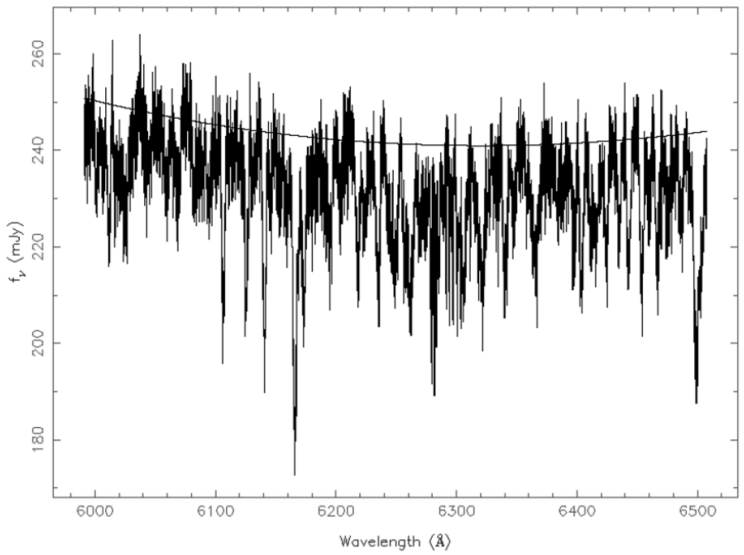

Fig.5: Spectrum with polynomial fit overlaid. The y-axis displays fluxf_ν, measured in millijanskys, mJy.

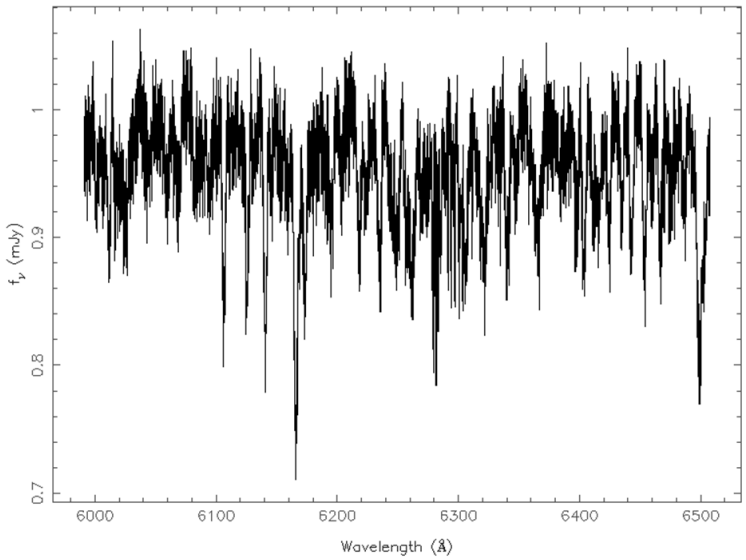

Fig. 6: Normalised spectrum after division by polynomial fit. The flux now is around 1mJy for most data points.

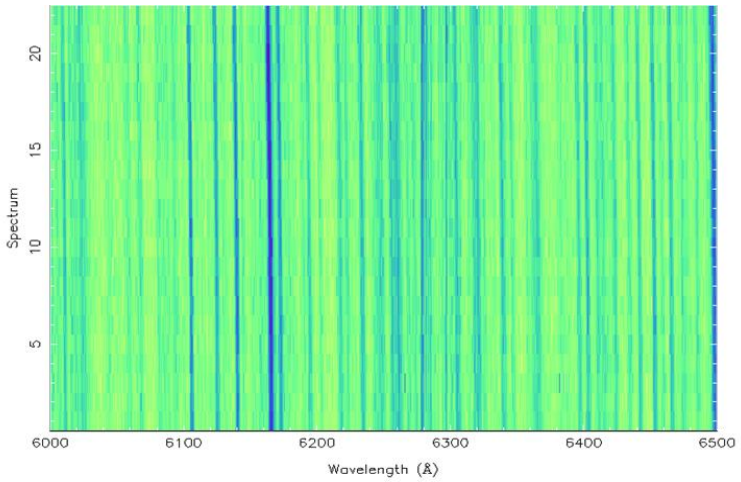

Fig. 7: Trail of all 22 spectra from night 1 after normalisation. The continuum variations have been removed as can be seen when compared with fig.4.

3.2 Estimation of *vsini*

An estimate for the rotational velocity *vsini* of the donor star requires an iterative process.
A non-rotating template of a star thought to be of similar spectral type is used which is a G8IV subgiant type star. This was chosen as the donor star in BV Cen is slightly evolved from the main sequence and has a low temperature of around 5000-6000K which matches this spectral template star.

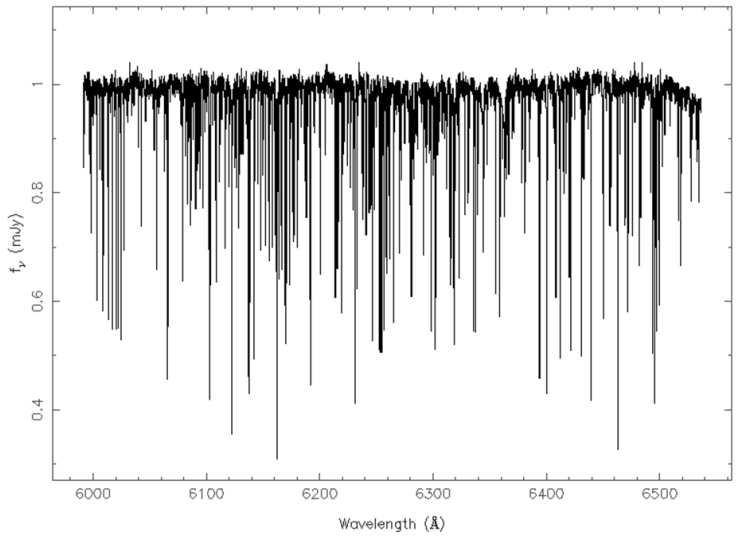

Fig.8: Normalised template spectrum (non-rotating)

The template and BV Cen spectra are normalised as described above and the continuum was set to zero by subtracting 1 from the flux. The spectra were placed onto a constant velocity scale using sinc function interpolation. This allowed the data, which is given in terms of wavelength, to be treated in velocity space.

A trial value for *vsini* of 100kms^{-1} was then used to artificially broaden the template spectrum to account for the rotational velocity of the donor star. A limb-darkening coefficient of 0.5 was assumed. This broadened template was then cross-correlated with the BV Cen spectra, calculating the radial velocity shifts between the two spectra throughout the orbit and producing a cross-correlation function for each spectrum. As this initial *vsini* value was an estimate, the results produced allow a first iteration on the radial velocity curve of the donor star.

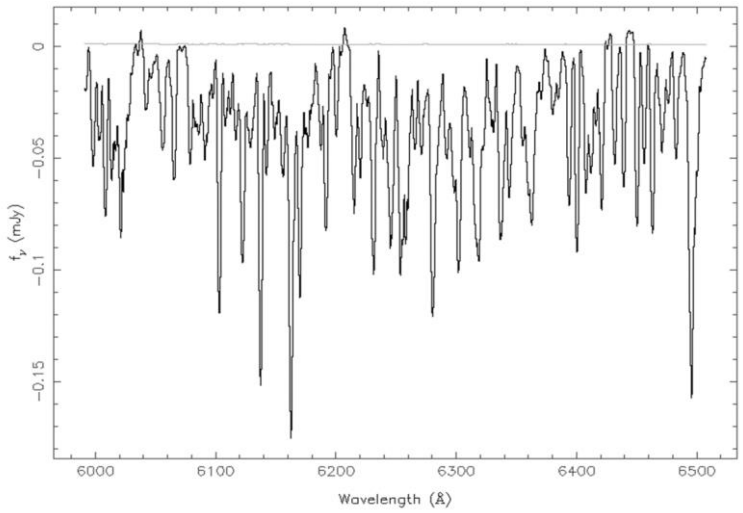

Fig.9: Template artificially broadened using *vsini* value of 100kms^{-1}. The broadening can be clearly seen in comparison with fig.8

The orbital motion of the donor star around the white dwarf is then removed from the spectra by subtracting the radial velocity shifts produced from the cross-correlation. In order to ensure the shifting took effect, the spectra were again rebinned onto the same velocity scale using sinc interpolation. The trails below show the spectra from each night before and after the orbital velocity is removed.

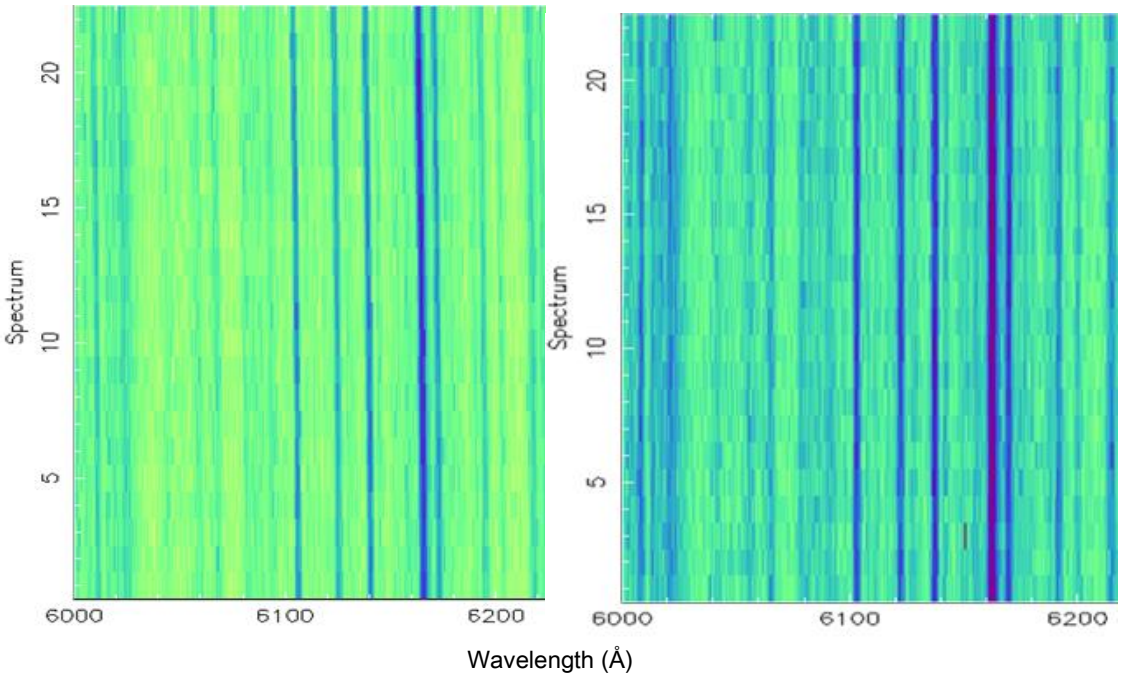

Fig.10 and Fig.11: Trail of night 1 spectra before and after correcting for orbital motion

The lines in the trail are now straight because the Doppler shifts due to orbital motion have been removed, therefore there is no shifting from spectrum to spectrum.

The BV Cen spectra were then averaged to produce an average spectrum for each night, which has been corrected for orbital motion. The template spectrum was then artificially broadened by trial *vsini* values in steps of 1kms^{-1} around the initial estimate of 100kms^{-1} and each broadened spectrum was saved.

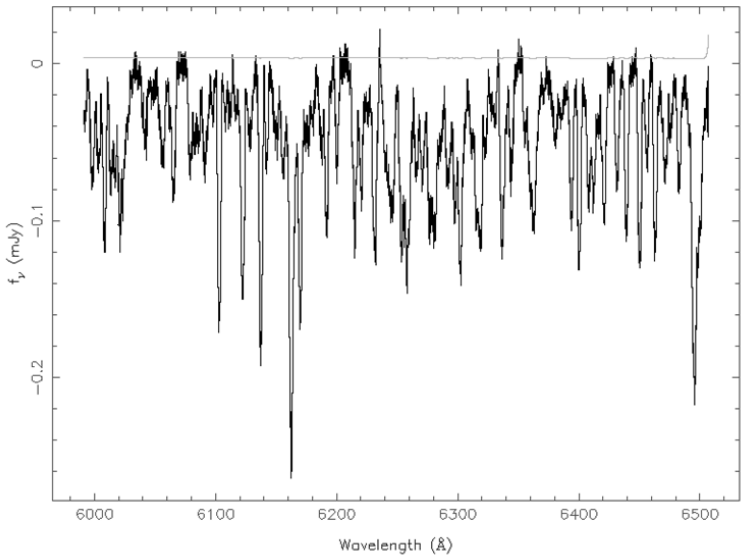

Fig.12: Average normalised continuum subtracted BV Cen spectrum for night 1

The average BV Cen spectrum was then compared with each broadened template spectrum by means of an optimal subtraction technique. The template spectra were each multiplied by a scale factor in order to match the average BV Cen spectrum then subtracted from it. The quality of the fit was measured by means of the χ^2 statistic.

$$\chi^2 = \sum_{i=1}^{N} \frac{(o_i - p_i)^2}{\sigma^2} \qquad \textit{Equation (2)}$$

Where: o_i is the observed data point
p_i is the predicted data point
σ is the uncertainty in the observed data point

The best *vsini* estimate minimised the χ^2 value and give the minimum scatter in the residual spectrum from the optimal subtraction process. Once the *vsini* value had been estimated the process was repeated, using this *vsini* value as the starting point for the next iteration. The process was repeated until the *vsini* value estimated at the start matched the value output at the end. This typically required 2 iterations.

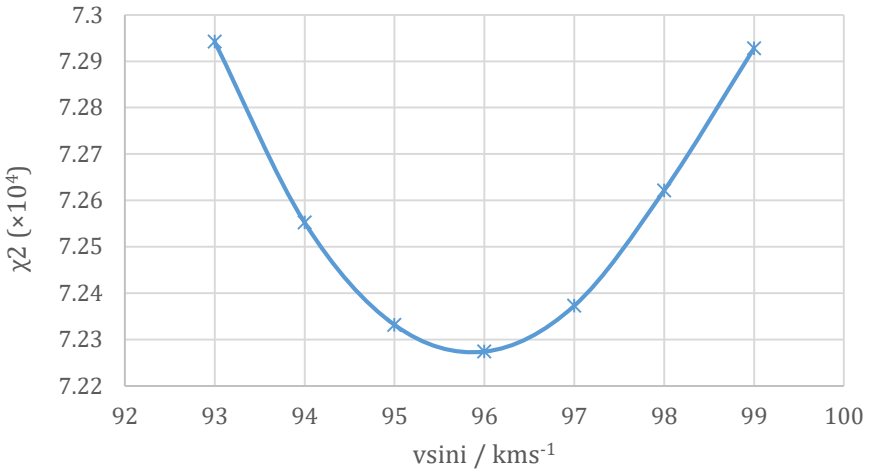

Fig.13: Chi squared values for night 1, showing the minimum at 96kms^{-1}

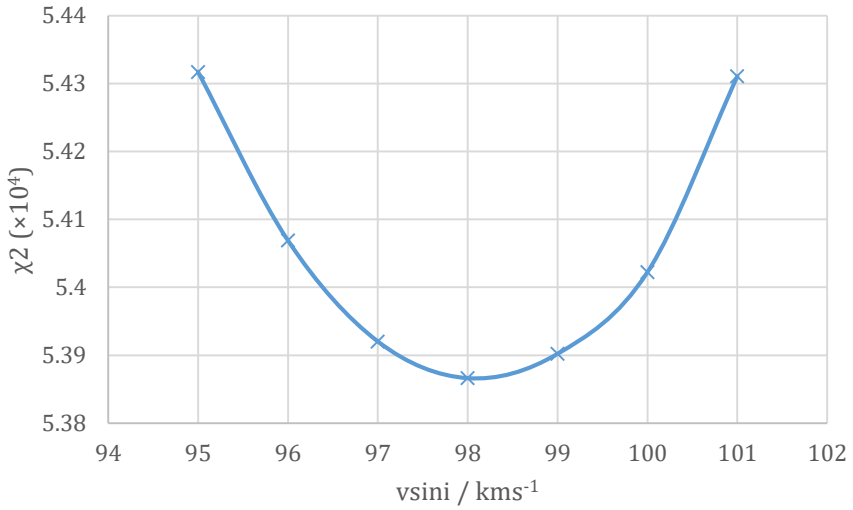

Fig 14: Chi squared values for night 2, showing the minimum at 98kms^{-1}

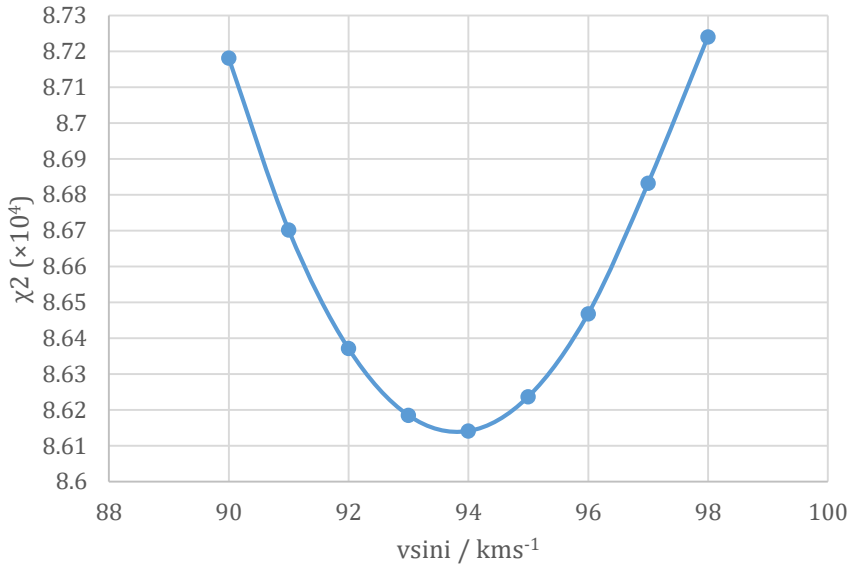

Fig.15: Chi squared values for night 3, showing the minimum at 94kms^{-1}

As fig.13 to 15 show, *vsini* was estimated to be 96kms^{-1} for night 1, 98kms^{-1} for night 2 and 94kms^{-1} for night 3. Therefore an average value for the rotational broadening of the donor star spectra over 3 nights was found to be (96.0 ± 2.0) kms^{-1}.

4. RADIAL VELOCITY CURVE OF DONOR STAR

As BV Cen is a tidally locked and synchronously rotating system, the projected equatorial rotation velocity, *vsini*, is related to the mass ratio q according to the equation:

$$\frac{V_{rot}sini}{R_L} = \frac{K_2+K_1}{a} = \frac{K_2(1+q)}{a} \qquad \textit{Equation (3)}$$

Where: a is the orbital separation.
R_L is the volume equivalent radius of the Roche Lobe- the radius of a spherical star with the same volume as the Roche Lobe. This is given by:

$$R_L = 0.47a\left(\frac{M_2}{M}\right)^{\frac{1}{3}} \qquad \textit{Equation (4)}$$

Where M is the total mass of the binary system.

Combining equations (3) and (4) gives:

$$Vsini = 0.47K_2q^{\frac{1}{3}}(1+q)^{\frac{2}{3}} \qquad \textit{Equation (5)}$$

Therefore the mass ratio can be estimated using a value for *vsini* and the radial velocity semi-amplitude of the donor star K_2. K_2 can be estimated using the radial velocity curve of the donor star.

The cross-correlation process used in determining *vsini* produced a file of radial velocity shifts and cross-correlation functions between the broadened template and each BV Cen spectrum. The radial velocity shifts produced for the final iteration for each night were used to produce a radial velocity curve by plotting the shifts as a function of orbital phase.

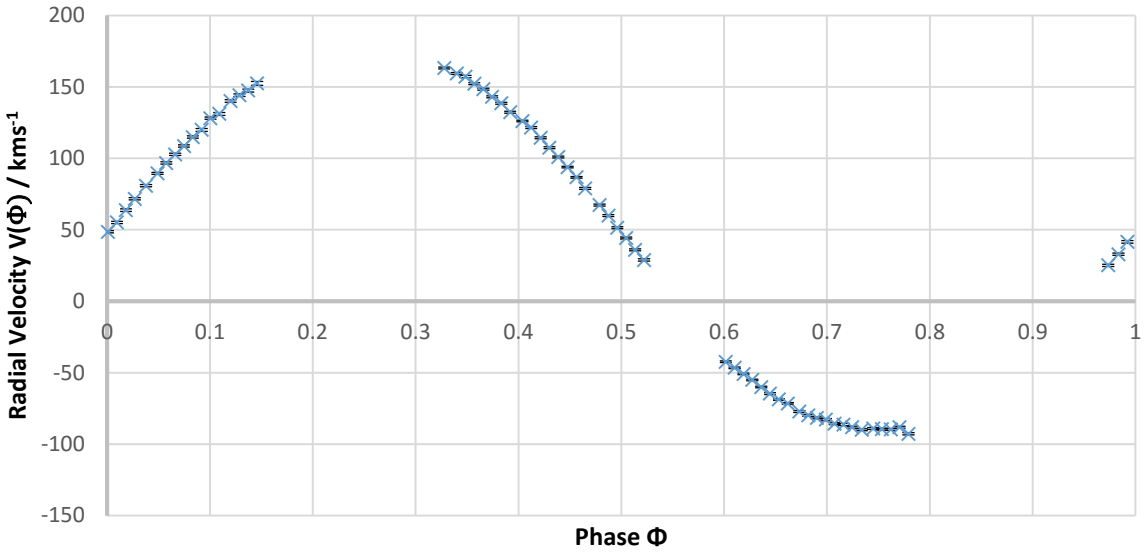

Fig.16: Radial Velocity Curve for BV Cen Donor Star

The curve can be fit by a sinusoid of the form:

$$V(\phi) = K_2 sin(2\pi\phi) + \gamma \qquad \textit{Equation (6)}$$

Where: $V(\Phi)$ is the radial velocity at orbital phase Φ

K_2 is the radial velocity semi-amplitude of the donor star

γ is the systemic velocity of the binary, the radial velocity of the system as a whole relative to the sun. Therefore the curve has a non-zero y-intercept.

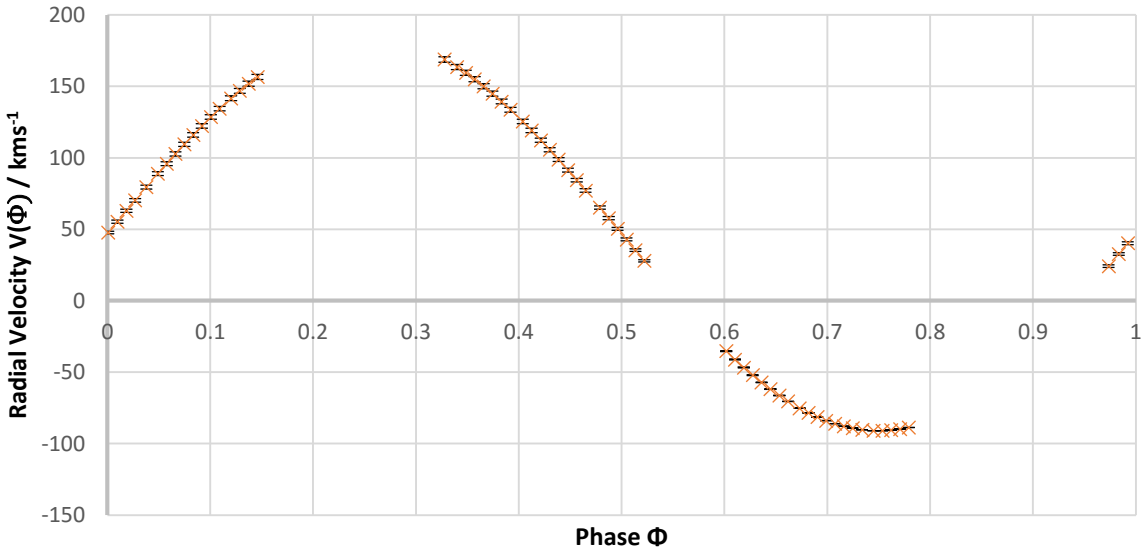

Fig.17: Sinusoid fitting to radial velocity curve of donor star

Predicted values for $V(\phi)$ were produced using equation (6) with initial estimates for K_2 and γ. A chi-squared test (equation (2)) was used between the observed data and the predicted data from the sinusoid fit.

The best fit was found by adjusting the values of K_2 and γ in intervals of 1kms^{-1} to in order to minimise the chi-squared statistic. When these values had been obtained they were then used in equation (5) along with the average $vsini$ value to find an estimate for the mass ratio q.

K_2 was found to be (138.0±1.0) kms^{-1} and γ was found to be (47±1.0) kms^{-1}. The true value of γ was calculated by adding the systemic velocity of the G8IV template star, (-67.24±0.10) kms^{-1} [1], giving a value of (-20.2±0.4) kms^{-1}.

Solving equation (5) for q, the mass ratio of the system was calculated to be q = (0.899±0.029).

The mass ratio estimate was used in equation (1) with a literature value for the mass of the donor star M_2 of (1.05±0.2)$M_\odot$ [1], giving an estimate for the white dwarf mass of M_1= (1.17±0.23)$M_\odot$.

5. RADIAL VELOCITY CURVE OF THE WHITE DWARF

The purpose of this process was to measure the radial velocity semi-amplitude of the white dwarf K_1, which could be used in equation (1) with the K_2 value estimated to produce another estimate of the mass ratio of the system q.

It is not possible to measure the radial velocity of the white dwarf directly. This is due to the fact that the white dwarf is obscured from view by the surrounding accretion disc. As the accretion disc orbits the white dwarf, the emission lines from the accretion disc can be traced and should reliably reflect the motion of the white dwarf.

In the BV Cen absorption spectra, a striking feature is the hydrogen alpha emission line at around 6562Å, as shown in fig.18.

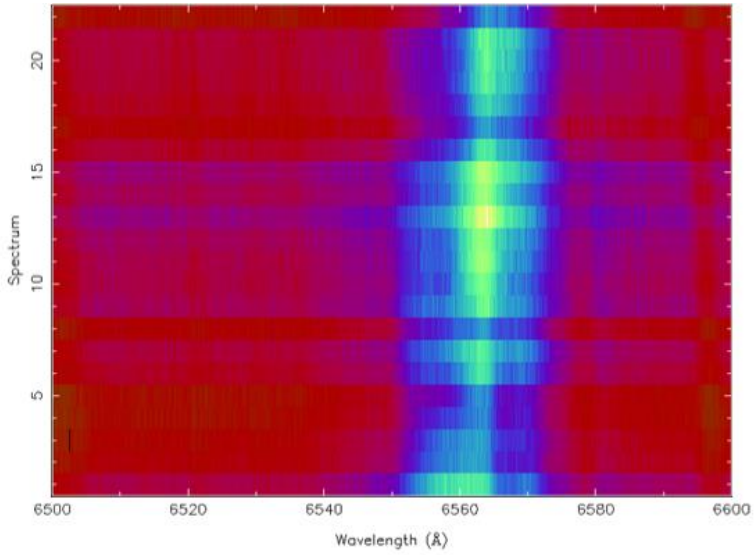

Fig. 18: Trail of spectra showing Hα emission line at around 6562Å.

The method to determine the radial velocity semi-amplitude was that outlined by Schneider [13] .
This method consists of convolving each spectrum with a pair of Gaussians of width σ whose centres have a separation of Δ. The position at which the intensities through the two Gaussians become equal is a measure of the wavelength of the emission line.

Two Gaussians were fit to this emission line in the range 6510-6600Å and the velocity offset of the centre of the two Gaussians was measured throughout the orbit.
The Gaussian widths were 200kms^{-1} with a separation of 400km^{-1}. The settings used were adjusted for each night. For all 3 nights the upper reject threshold was set to 4σ. For nights 1 and 2 a lower reject threshold of -2σ was used and for night 3 -1.8σ was used.

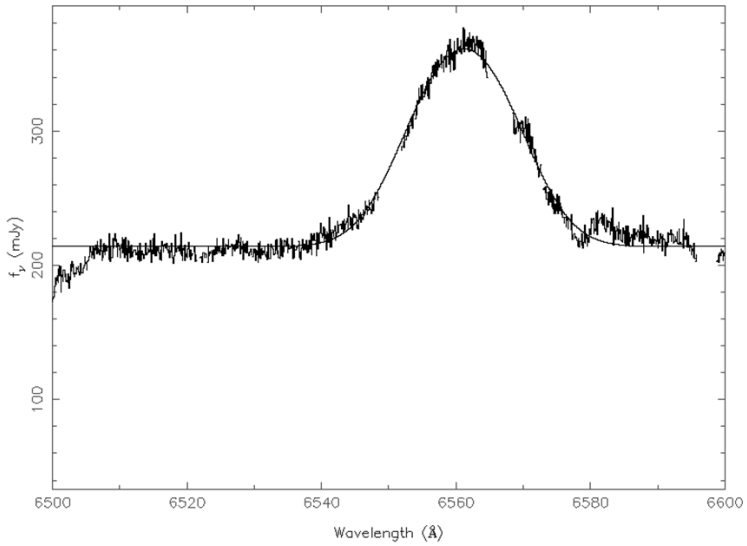

Fig.19: Two Gaussians fit to Hα emission line in range 6510 to 6600Å

For each BV Cen spectrum the velocity offset corresponding to the central wavelength of the two Gaussians was used to produce a radial velocity curve.

This curve can be fit by a sinusoid of the form:

$$V(\phi) = K_1 sin(2\pi\phi + \theta) + \gamma \qquad \textit{Equation (7)}$$

Where: K_1 is the radial velocity semi-amplitude of the white dwarf
γ is the systemic velocity of the white dwarf
θ is the offset from phase zero at the limit between redshift and blueshift

As before the values of K_1, γ and θ were adjusted to find the best fit by means of a chi-squared test. The value of K_1 could then be used with the previously calculated K_2 in equation (1) to provide another estimate for the mass ratio.

K_1 was found to be (-126.0±1.0) kms^{-1}
γ was found to be (-121±1.0) kms^{-1}
θ was found to be (346.0±1.0)°=(1.922±0.006)π radians

The radial velocity curve and sinusoidal fit are shown below.

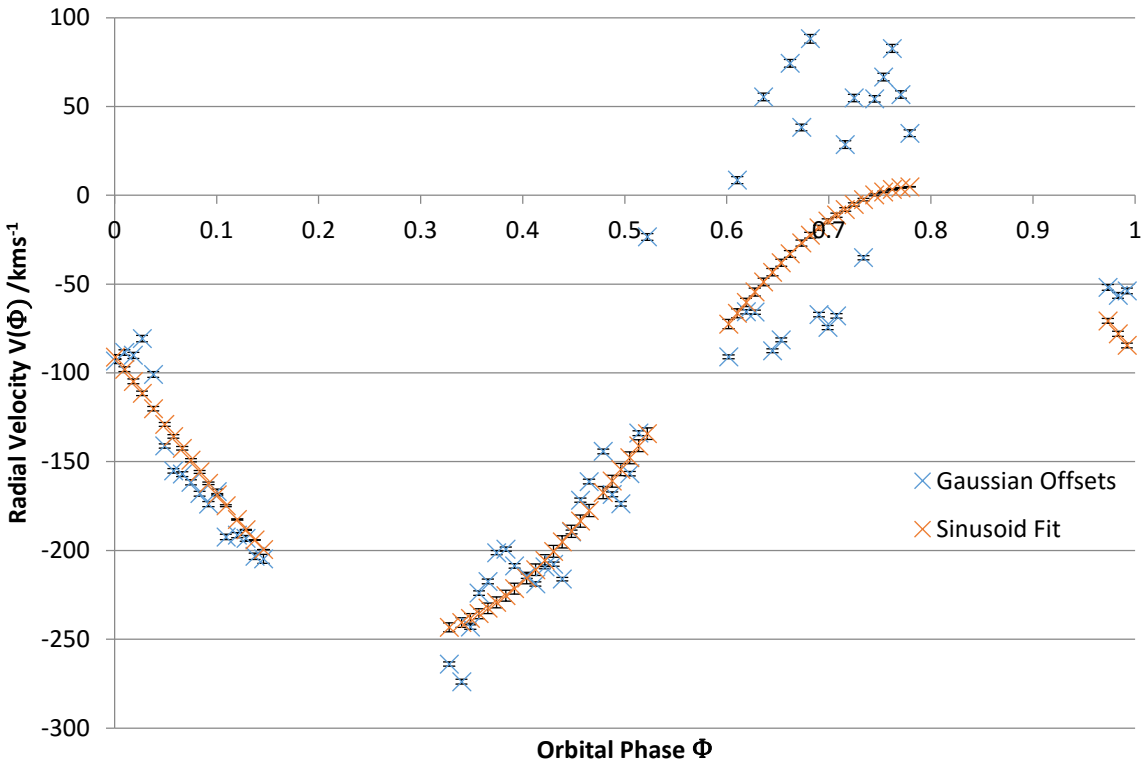

Fig.20: Radial velocity curve of white dwarf using Gaussian fittings to H alpha emission line

The uncertainty in the predicted radial velocities in the sinusoid fit arise due to the errors in K_1, γ and θ. The values of K_2 and γ were adjusted in steps of ±1kms^{-1} , and θ was adjusted in steps of ±1° then converted to radians for the chi-squared calculation.

Therefore the mass ratio can be estimated:

$$q = \frac{K_1}{K_2} = \frac{(126.0 \pm 1.0)}{(138.0 \pm 1.0)} = (0.91 \pm 0.01) = \frac{M_2}{M_1}$$

The uncertainty in the mass ratio was calculated from the propagation of errors formula,

$$\left(\frac{\delta q}{q}\right)^2 = \left(\frac{\delta K_1}{K_1}\right)^2 + \left(\frac{\delta K_2}{K_2}\right)^2 \qquad \textit{Equation (8)}$$

As before the estimate for the mass ratio was used with the literature value for the donor star mass giving an estimate for the white dwarf mass of $(1.15 \pm 0.22) M_{\odot}$.

Therefore the sinusoid fits can be plotted on the same graph to give a radial velocity curve for the binary system as a whole.

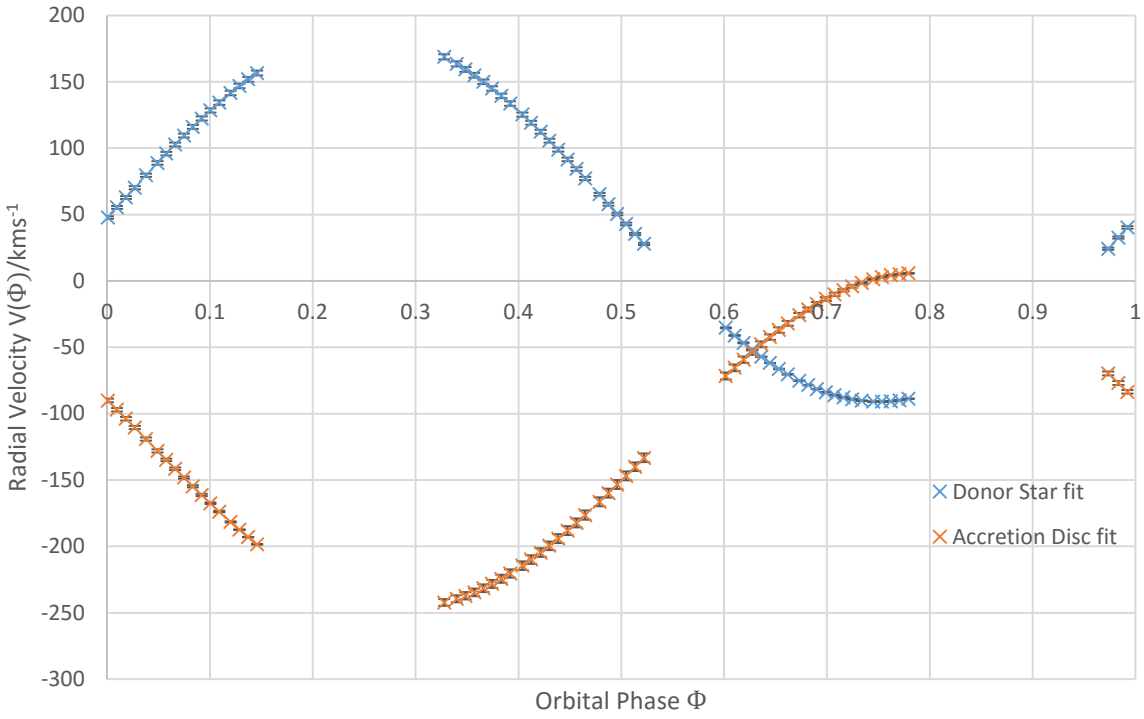

Fig.21: Sinusoid fits for donor star and white dwarf radial velocity curves

6. DISCUSSION OF RESULTS AND CONCLUSIONS

Using the rotational broadening and the radial velocity curve of the donor star in BV Cen, $vsini$ was found to be (96.0±2.0) kms^{-1}. The mass ratio was found to be (0.899±0.029) and therefore the mass of the white dwarf was estimated to be (1.17±0.23)$M_{\odot}$. The systemic velocity of the system was estimated to be (-20.2±0.4)kms^{-1}. These results agree with literature values from estimates by Watson et al [1] of (1.18±0.28)$M_{\odot}$and γ =(-20.3±0.2) kms^{-1} to within the stated uncertainties.

However when using radial velocity techniques, homogenous stellar structure is assumed. Watson et al [1] also used the entropy landscape method to calculate the systemic velocity of BV Cen, yielding a value of γ= -22.3kms^{-1}. This technique examined the entropy of the system as a function of systemic velocity. Our value derived from radial velocity analysis only differs from this value by 2.1 kms^{-1}, suggesting that either inhomogeneities on the surface of BV Cen have little impact on the radial velocity or that irradiation of BV Cen is fairly low and not large enough to cause a clear discrepancy in the values. Therefore in a binary system where irradiation is greater than in BV Cen there could be a greater difference in results.
The experimental value for $vsini$ could be improved by using estimates for $vsini$ in the optimal subtraction process in intervals of 0.1 kms^{-1} instead of 1 kms^{-1}. This would lead to a greater accuracy when finding a value for the mass ratio.

By fitting Gaussians to the hydrogen alpha emission line and measuring the offsets throughout the orbit, another estimate for the mass ratio was found to be (0.91±0.01) and the white dwarf mass (1.15±0.22)$M_{\odot}$. These results are in relative agreement with those calculated using the radial velocity curve of the donor star. However this method has inaccuracies due to low signal to noise from the accretion disc which can be shown by the scatter in the data points and the high χ^2 squared value of 34033.1 when fitting the sinusoid.
These results could have been improved by fitting Gaussians to other emission lines, such as He I emission at around 5876Å. This would have allowed offsets to be measured for multiple emission lines and therefore allow a more accurate estimate for the mass ratio.

When using Keplerian motion equations it is assumed that the system can be treated as a two-body problem. However this may not be the case in a binary system with an accretion disc due to large amounts of mass being transferred.

An accepted value for the mass of an isolated white dwarf is $0.7M_{\odot}$ [10]. Therefore the calculated values for M_1 shows that the BV Cen white dwarf has gained mass via accretion and suggests that it could reach Chandrasekhar mass. The results therefore suggest that BV Cen, and by extension dwarf novae, may possibly be SNIa progenitors. However due to nova and dwarf nova eruptions the white dwarf may lose mass more rapidly than it gains mass, preventing it from reaching M_{Ch}. Therefore the evidence put forward in this report may not be regarded as definitive evidence for a type 1a progenitor, and could only be regarded as such if BV Cen had been observed exactly as it reached Chandrasekhar mass and commenced gravitational collapse.

REFERENCES

1. *Roche tomography of cataclysmic variables--IV. Star-spots and Slingshot Prominences on BV Cen*-Watson, CA, Steeghs, D, Shahbaz, T and Dhillon, VS, Monthly Notices of the Royal Astronomical Society Volume 382, Number 3, p1105-1118, 2007

2. *Classification of supernovae*-Turatto, M, Supernovae and Gamma-Ray Bursters, p21-36, 2003

3. *The absolute magnitudes of Type IA supernovae*-Phillips, M, The Astrophysical Journal, Volume 413, L105-L108, 1993

4. *Progenitors of type Ia supernovae*-Wang, Bo and Han, Zhanwen, New Astronomy Reviews, Volume 56, Number 4, p122-141, 2012

5. *The physics of type Ia supernovae*-Thielemann, F-K, Brachwitz, F, Hoflich, P, Martinez-Pinedo, G and Nomoto, K, New Astronomy Reviews, Volume 48, Number 7, p605-610, 2004

6. *Astronomy-A Physical Perspective*-M.L.Kutner, Second Edition, p189

7. *CI Aql: a Type Ia supernova progenitor?*-Sahman, DI, Dhillon, VS, Marsh, TR, Moll, S, Thoroughgood, TD, Watson, CA and Littlefair, SP, Monthly Notices of the Royal Astronomical Society, 2013

8. *Recurrent novae as a progenitor system of type Ia supernovae. I. RS Ophiuchi subclass: systems with a red giant companion*-Hachisu, I and Kato, M, The Astrophysical Journal, Volume 558, Number 1, 323, 2001

9. *An Introduction to the Theory of Stellar Structure and Evolution*-Prialnik, D, Second Edition, p223-229

10. *Introductory Astronomy and Astrophysics*- Zeilik, Gregory, Second Edition, p334

11. Magellan Telescopes –*http://www.lco.cl/telescopes-information/magellan/telescopes-information/magellan/* accessed on 01.05.2016

12. *Optical astronomical spectroscopy*- Kitchin, Christopher R, p202-3, 216-220, 1995

13. *Interpreting astronomical spectra*- Emerson, D, p77-83, 1996

14. "The magnetic maw of 2A 0311-227." - Schneider, D, Young, The Astrophysical Journal 238, p946-954, 1980